2023 IEEE International Conference on Robotics and Automation (ICRA 2023)
May 29 - June 2, 2023. London, UK

Adaptive based Assist-as-needed control strategy for Ankle movement assistance

R. Jradi, H. Rifaï, Y. Amirat, S. Mohammed[1]

Abstract— **Stroke affects a large number of people every year. One consequence is the weakness of ambulatory muscles resulting in a paretic gait. Actuated ankle foot orthoses can be a solution to assist paretic patients to dorsiflex and/or plantar flex their ankle joint during the gait phases. To assist the wearer following a predefined ankle joint desired trajectory, an adaptive active disturbance rejection controller is proposed in this study. The human muscular torque and estimation errors are estimated through a nonlinear disturbance observer based on the estimated model. This estimated torque is compensated within the proposed projection based adaptive controller combined to a saturated proportional derivative term. The purposes of using this controller are : i) the no need of prior system's parameter identification due to the adaptive structure, ii) the assistance-as-needed of the wearer through the rejection term and iii) the avoidance of the actuator saturation by including projection and saturation functions. This controller is tested in real time using an actuated ankle-foot-orthosis (AAFO) in lab environment with three healthy subjects to show its effectiveness.**

I. INTRODUCTION

Stroke is among the leading causes of disability around the world. The number of stroke survivors per year is estimated at fifteen million in the world and over one hundred and forty thousand in France. According to the french national institute of health and medical research (INSERM) [1], about 40 % of the survivors suffer significant sequelae. One of the major consequences is the neuromuscular disorder. It may result in hemiplegia i.e. limb paralysis, hemiparesis i.e. muscle weakness or ataxia i.e. lack of coordination, affecting the daily living activities of the patients. Depending on the degree of impairment, the patient should undergo rehabilitation sessions to regain movement or even autonomy. Classically, the rehabilitation is performed by therapists who assist the patient in performing repetitive movements of the affected limb. However, this task is often difficult and painful for both patient and therapist doctors. Thus, actuated robotic orthoses/exoskeletons appear to be an appropriate solution to provide assistance to the patient on the one hand [1], and relax the therapist from the relatively important efforts on the other hand. These rehabilitation sessions using wearable robots should be supervised by a therapist who ensures the safety of the wearer, checks his state of progress and the achievement of the rehabilitation goals.

Lower limb exoskeleton development has increased in the last decades and is intended for several purposes. Two main applications are i) the force augmentation dedicated to industrial or military applications and ii) the rehabilitation/assistance of elderly and spinal cord injured or stroke patients. The mechanical structure of the exoskeleton should be lightweight, easy to don and doff and fit perfectly the morphology of the wearer [2]. Recent developed structures include soft or flexible elements to generate more natural movements [3], [4], [5] or additive manufacturing using smart materials [6]. Different control strategies have been developed to ensure transparent interaction between the wearer and the exoskeleton. EMG-based controllers ensure the control of the exoskeleton using the measurement of the electromyographical activities [7], [8]. Often, the torque delivered by the exoskeleton's actuator is an amplification of the EMG's measurements. These controllers present some limitations due to the fact that the EMG measurements are affected by the position of the sensors, the skin impedance, the muscular fatigue and the amplitude of the measured EMG signal that depends on the impairment degree [9]. Impedance control has been also widely used for exoskeletons [10], [11], [12], [13], [14]. It allows setting the impedance of the wearer-exoskeleton system to a desired level corresponding to a movement requirement e.g. in terms of stiffness, damping, etc. Within this strategy, the system's parameters should be beforehand accurately identified. Besides, the movement should be voluntarily initiated by the wearer. Another control strategy consists on tracking a desired trajectory of a given joint [15], [16], [17], [18], [19]. This control strategy is adapted to people not able to initiate any movement.

The present study focuses on the gait impairment of hemiparetic patients as a targeted population. These patients are not able to sufficiently dorsiflex and/or plantar flex their ankle joint at some key moments of the gait cycle. To support these patients, an actuated ankle-foot orthosis can be used to assist the ankle dorsiflexion during the foot landing and the ankle plantar flexion during the foot taking off [20]. The different sub-phases of the gait cycle have been identified online and an adaptive reference trajectory of the ankle joint has been proposed in previous work [19]. In this paper, an adaptive active disturbance rejection control is applied to the orthosis actuator to assist the wearer performing a normal gait by tracking the adaptive reference trajectory. The controller includes three main terms : i) a projection based adaptive control law, ii) a saturated proportional derivative controller and iii) a rejection term characterizing the estimation of the human muscular torque by means of a nonlinear disturbance observer. On the one hand, the proposed controller does not require any prior identification of both wearer and orthosis'

[1]Univ Paris Est Creteil, LISSI, F-94400 Vitry, France {rami.jradi, hala.rifai, amirat, samer.mohammed}@u-pec.fr

1. https://www.inserm.fr , Accessed : September 2022.

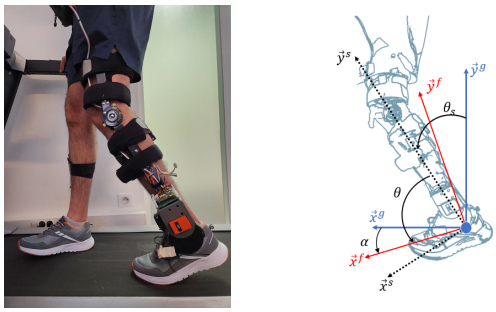

(a) (b)

FIG. 1 – The foot frame $\mathcal{F}(\vec{x}^f, \vec{y}^f, \vec{z}^f)$ is attached to the foot at the ankle level with $\vec{x}^f$ in the heel-half of the insole plane. The ground frame $\mathcal{G}(\vec{x}^g, \vec{y}^g, \vec{z}^g)$ is fixed. The angle θ_s determines the orientation of the shank relative to the vertical axis, α gives the orientation of the foot relative to the longitudinal axis and θ is the angle between the foot and the shank.

parameters. On the other hand, the rejection term allows to compensate the estimated human muscular torque to provide the wearer with only the required assistance to perform a given movement. The saturation and projection functions ensure the boundedness of the control torque, avoid the saturation of the actuator and emphasize its performance in linear regime which helps preserving the safety of the wearer. Experimental results are performed by three healthy subjects using the actuated ankle-foot orthosis (AAFO) in lab environment to show the effectiveness of the the proposed controller.

The paper is structured as follows : in section II, the model of the AAFO-wearer system is presented. The adaptive reference trajectory is also shortly described. In section III, the active disturbance controller is presented including the nonlinear disturbance observer and the adaptive controller. The stability analysis of the closed loop wearer-orthosis system is developed in section IV. The preliminary experimental results are shown in section V. Finally, the conclusions and future works are addressed in section VI.

II. SYSTEM MODELLING

A. Model of the actuated-ankle-foot-orthosis system

The Actuated Ankle Foot Orthosis (AAFO) has one rotational degree of freedom at the ankle joint level and one passive degree of freedom at the knee joint level. It is embodied by the shank and the foot and the set is considered as one entity called the AAFO system. A schematic of the AAFO system is given in FIG. 1. Two frames are defined : $\mathcal{F}(\vec{x}^f, \vec{y}^f, \vec{z}^f)$ attached to the foot such that $\vec{x}^f$ has the same direction as the foot and $\mathcal{G}(\vec{x}^g, \vec{y}^g, \vec{z}^g)$ a fixed frame where $\vec{x}^g$ has the longitudinal direction, $\vec{y}^g$ the vertical one and $\vec{z}^g$ defined such that the three-sided frame is direct. Let θ be the angle between the foot and the shank, θ_s the angle between the shank and the vertical axis. θ and θ_s are measured using the embedded sensors of the AAFO system. Define α as the angle between the foot and the longitudinal direction, it is given by : $\alpha = \theta_s + \theta - \frac{\pi}{2}$.

During a walking cycle, the AAFO system is subject to the friction torque (solid and viscous) noted $\tau_f = -A\text{sign}\dot{\theta} - B\dot{\theta}$, the torque induced by the translational acceleration of the foot $\tau_a = -C(a_y \cos\alpha - a_x \sin\alpha)$, the joint stiffness torque $\tau_s = -K(\theta - \theta_r)$, the torque induced by the ground reaction force $\tau_r = -(R_1x_1 - R_2x_2 - R_3x_3)\cos\alpha$, the torque resulting from the gravity of the foot $\tau_{\text{gravity}} = -\tau_g \cos\alpha$, the torque generated by the muscules actuating the ankle joint τ_h and the torque developed by the AAFO's actuator τ. The rotational dynamics of the AAFO-system can be written as :

$$\begin{aligned} J\ddot{\theta} &= \tau_f + \tau_a + \tau_s + \tau_r + \tau_{gravity} + \tau_h + \tau \\ J\ddot{\theta} &= -A\text{sign}\dot{\theta} - B\dot{\theta} - C(a_y \cos\alpha - a_x \sin\alpha) \\ &\quad -K(\theta - \theta_r) - \gamma(R_1x_1 - R_2x_2 - R_3x_3)\cos\alpha \\ &\quad -\tau_g \cos\alpha + \tau_h + \tau \end{aligned} \quad (1)$$

where θ, $\dot{\theta}$, $\ddot{\theta}$ are respectively the rotational angle, angular velocity and acceleration of the ankle joint, θ_r is the ankle joint angle at the rest position of the foot, a_x and a_y are respectively the longitudinal and vertical acceleration of the translational movement, R_1, R_2, R_3 are the ground reaction forces at the heel, middle and toes levels, x_1, x_2, x_3 are the positions of the force sensing resistors embedded in the insoles. A, B, C, K, γ and τ_g are respectively the solid friction, viscous friction, acceleration, stiffness, ground reaction force and gravity system's parameters. sign is a signum function.

B. Adaptive reference trajectory

The gait cycle is divided into two main phases [21] : the stance phase when the foot is in contact with the ground and the swing phase when there is no contact with the ground (FIG. 2). The stance phase can be further divided into five sub-phases : loading response (LR), early-mid-stance (EMS) and late-mid-stance (LMS), terminal stance (TS) and pre-swing (PS). The swing phase can further be divided into three sub-phases based on the state of the opposite foot : initial swing (ISw), mid-swing (MSw) and terminal swing (TSw).

Three force sensitive resistors (FSR) placed in each of the insoles of the feet and an Inertial Measurement Unit (IMU) placed at the shank level of the left leg contributed to detect accurately the initial contact event (FIG. 2). Then, a standard Mamdani fuzzy inference system is applied to detect the gait sub-phases based on the outputs of the FSR sensors and the IMU [22], [23]. Based on the detected gait events, an ankle joint angle reference is adaptively generated, with respect to the wearer's walking speed, step length and gait events (FIG. 2). The corresponding reference is based on the average ankle joint angle of 20 healthy subjects recorded in [24], it ensures the gait correction toward a healthy one. For further information about the sub-phases detection and the reference trajectory generation, the reader is invited to refer to [19].

III. ACTIVE DISTURBANCE REJECTION CONTROLLER

The main purpose of this paper is to develop a controller that can be adapted to different wearers without the need to estimate the system's (orthosis and wearer) parameters before each experiment. Another purpose is to provide the necessary

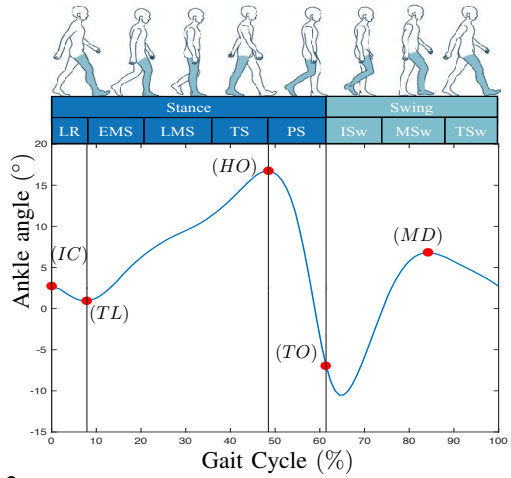

FIG. 2 – On the top, the gait cycle phases : stance and swing and sub-phases : LR=Loading Response, EMS=Early Mid-Stance, LMS=Late Mid-Stance, TS=Terminal Stance, PS=Pre-Swing, ISw=Initial Swing, MSw=Mid-Swing, TSw=Terminal Swing. On the bottom, the events in the gait cycle that trigger a transition at some gait sub-phases : IC=Initial Contact, TL=Toe Landing, HO=Heel Off, TO=Toe off, MD=Maximum dorsiflexion. The ankle angle is measured from the relaxed ankle angle, such that the positive values are considered dorsiflexion and the negative values are plantar-flexion.

amount of assistance to the wearer. For these purposes, a nonlinear disturbance observer is developed to estimate the human muscular torque developed by the wearer to ensure the movement. The remaining needed amount of assistance is provided by the orthosis actuator. It is based on two main terms : i) a Projection-Based Model Reference Adaptive Controller (PB-MRAC) and ii) a Saturated Proportional Derivative (SPD) controller. The active disturbance rejection controller is composed of the PB-MRAC-SPD controllers and a compensation of the estimated human muscular torque. The orthosis' torque is intended to drive the AAFO to track an adaptive reference ankle joint trajectory. Let θ_d, $\dot{\theta}_d$ and $\ddot{\theta}_d$ denote the desired angle, angular velocity and acceleration of the ankle joint. Define $s = \dot{\tilde{\theta}} + \lambda\tilde{\theta}$ where λ is a scalar positive parameter, $\tilde{\theta} = \theta - \theta_d$ and $\dot{\tilde{\theta}} = \dot{\theta} - \dot{\theta}_d$.

Assumption 1: The current and desired ankle joint angles and their derivatives up to the second order $(\theta, \dot{\theta}, \ddot{\theta}, \theta_d, \dot{\theta}_d, \ddot{\theta}_d)$ are considered well known and bounded.

Denote by W the vector of the system's parameters : $W = [A,\ B,\ C,\ K,\ J,\ \gamma, \tau_g] \in \mathbb{R}^{1\times 7}$ and $\hat{W}$ the vector of the estimated ones :

$$\hat{W} = [\hat{A},\ \hat{B},\ \hat{C},\ \hat{K},\ \hat{J},\ \hat{\gamma}, \hat{\tau_g}] \tag{2}$$

The parameters estimation error vector is defined as : $\tilde{W} = W - \hat{W}$ and its derivative : $\dot{\tilde{W}} = -\dot{\hat{W}}$, assuming that the system's parameters remain constant.
Denote by $Y \in \mathbb{R}^{1\times 7}$ the vector :

$$\begin{aligned} Y =& [\text{sign}\dot{\theta},\ \dot{\theta},\ (a_y \cos\alpha - a_x \sin\alpha),\ (\theta - \theta_r),\ (\ddot{\theta}_d - \lambda\dot{\tilde{\theta}}),\\ & (R_1 x_1 - R_2 x_2 - R_3 x_3)\cos\alpha,\ \cos\alpha] \end{aligned} \tag{3}$$

Replacing (2) and (3) into (1), the dynamics of the system can be written as :

$$J\dot{s} = -WY^T + \tau + \tau_h \tag{4}$$

that is :

$$\underbrace{J\dot{s} + WY^T}_{f(\theta,\dot{\theta},\ddot{\theta},\theta_d,\dot{\theta}_d,\ddot{\theta}_d)} = \tau + \tau_h \tag{5}$$

Consider the estimated dynamics of the system as :

$$\hat{f}(\theta, \dot{\theta}, \ddot{\theta}, \theta_d, \dot{\theta}_d, \ddot{\theta}_d) = \hat{J}\dot{s} + \hat{W}Y^T \tag{6}$$

The dynamics of the system can be written as the sum of the estimated dynamics $\hat{f}$ and estimation error $\tilde{f}$ as :

$$f(\theta, \dot{\theta}, \ddot{\theta}, \theta_d, \dot{\theta}_d, \ddot{\theta}_d) = \hat{f}(\theta, \dot{\theta}, \ddot{\theta}, \theta_d, \dot{\theta}_d, \ddot{\theta}_d) + \tilde{f}(\theta, \dot{\theta}, \ddot{\theta}, \theta_d, \dot{\theta}_d, \ddot{\theta}_d) \tag{7}$$

For sake of simplicity, the embedded parameters of the functions f, $\hat{f}$ and $\tilde{f}$ are removed on the sequel. Then, the estimated dynamics can be written as :

$$\hat{J}\dot{s} + \hat{W}Y^T = \tau + \tau_h - \tilde{f} \tag{8}$$

Consider d as external input of the estimated AAFO system model : $d = \hat{J}^{-1}\big(\tau_h - \tilde{f}\big)$.

$$\hat{J}\dot{s} + \hat{W}Y^T = \tau + \hat{J}d \tag{9}$$

Remark 1: The human muscular torque τ_h spanning the ankle joint is bounded by Δ_h : $|\tau_h| \leq \Delta_h$.

Assumption 2: The external input d of the estimated AAFO system model is considered bounded up to its first derivative, i.e. $|d| < B_d$ and $|\dot{d}| < B_{\dot{d}}$. It results from Remark 1 that the estimation error $\tilde{f}$ is also bounded, i.e. $|\tilde{f}| < B_{\tilde{f}}$.

A. *Estimation of external torque and estimation errors*

A nonlinear disturbance observer (NDOB) is developed to estimate the external input d of the estimated AAFO-wearer model. The estimated input is denoted $\hat{d}$ and is given by :

$$\begin{aligned} \dot{z} &= -l(s,Y)z - l(s,Y)\big(p(s,Y) + \hat{J}^{-1}(\tau - \hat{W}Y^T)\big) \\ \hat{d} &= z + p(s,Y) \end{aligned} \tag{10}$$

where $z \in \mathbb{R}$ is the internal state of the disturbance observer, $p(s,Y)$ and $l(s,Y)$ are respectively function and gain to be designed. Let $\tilde{d}$ be the external input estimation error : $\tilde{d} = d - \hat{d}$. The dynamics of the the external input estimation error are given by :

$$\dot{\tilde{d}} = \dot{d} + l(s,Y)\Big(z + p(s,Y) + \hat{J}^{-1}\big(\tau - \hat{W}Y^T\big)\Big) - \dot{p}(s,Y)$$

By substituting (9) and (10), the dynamics of the external input estimation error become :

$$\dot{\tilde{d}} = \dot{d} - l(s,Y)\tilde{d} + l(s,Y)\dot{s} - \dot{p}(s,Y) \tag{11}$$

Proposition 1: Consider the AAFO system estimated model (9). Considering $l(s,Y) = L \in \mathbb{R}_+$ and $p(s,Y) = Ls$, the nonlinear disturbance observer (10) ensures the estimation of the external input d, and the trajectories of the observer estimation error remain ultimately bounded.

Proof: By considering $l(s,Y) = L \in \mathbb{R}_+$ and $p(s,Y) = Ls$, the dynamics of the external input estimation error become :

$$\dot{\tilde{d}} = \dot{d} - L\tilde{d} \tag{12}$$

Consider the Lyapunov candidate function :

$$T = \frac{1}{2}\tilde{d}^2 \tag{13}$$

The derivative of the Lyapunov function T is given by :

$$\dot{T} = \dot{d}\tilde{d} - L\tilde{d}^2$$

Considering Assumption 2, the derivative of the Lyapunov function T can be bounded by :

$$\dot{T} \leq -L\tilde{d}^2 + B_{\dot{d}}|\tilde{d}| \tag{14}$$

Hence, $\dot{T} \leq 0$ outside the set $\{|\tilde{d}| \leq B_e\}$ where $B_e = \frac{1}{L}B_{\dot{d}}\}$. Considering $T_M > \frac{1}{2}B_e^2$, solutions starting in the set $\{T \leq T_M\}$ will remain therein for all future time since $\dot{T} < 0$ on the boundary $T = T_M$. Therefore, the solutions are uniformly bounded for any ϵ such that $\frac{1}{2}B_e^2 < \epsilon < T_M$. $\dot{T}$ is negative in the set $\{\epsilon < T < T_M\}$ which means that T will decrease monotonically until the solution enters the set $\{T < \epsilon\}$ where it cannot leave. Therefore, the solution is uniformly ultimately bounded with the ultimate bound equal to $\sqrt{2\epsilon}$. ■

B. Projection-based adaptive control with saturated proportional derivative term

The proposed PB-MRAC-SPD control torque has the following expression :

$$\tau = \hat{W}Y^T - \alpha_p \text{sat}_{N_1}(k_p\tilde{\theta}) - \alpha_v \text{sat}_{N_2}(k_v\dot{\tilde{\theta}}) - \hat{J}\hat{d} \tag{15}$$

where $\alpha_p,\ \alpha_v,\ k_p,\ k_v$ are scalar positive gains and N_1, N_2 the bounds of the proportional and derivative actions. $\hat{d}$ is the external input estimation determined by (10). $\text{sat}_N(\cdot)$ is a saturation function, bounded between $\pm N$, defined such as :

$$\text{sat}_N(x) = \begin{cases} x & \text{if} \quad |x| \leq N \\ N\text{sign}(x) & \text{if} \quad |x| > N \end{cases} \tag{16}$$

with $x \in \mathbb{R}$ and $\text{sign}(\cdot)$ the classical sign function.

The parameters adaptation law is given by :

$$\dot{\hat{W}} = -\Gamma \text{Proj}(Y^T s, \hat{W}) \tag{17}$$

where Y and $\hat{W}$ are defined in (3, 2) and Γ is a positive definite scaling diagonal matrix : $\Gamma = \text{diag}(\Gamma_i)$, $i \in \{1, \ldots, 7\}$. $\text{Proj}(y, \hat{W})$ is a projection operator defined in [25]. The projection operator is given by :

$$\text{Proj}(y,\hat{W}) = \begin{cases} y & \text{if } ||\hat{W}|| < W_M \text{ or } \hat{W}^T y \geq 0 \\ (I - \frac{\hat{W}\hat{W}^T}{||\hat{W}||^2})y & \text{if } ||\hat{W}|| \geq W_M \text{ and } \hat{W}^T y < 0 \end{cases} \tag{18}$$

Remark 2: Note that the estimated parameters through (17) do not represent their true corresponding values. They are estimated to compute the assistive torque such that it ensures the best possible tracking.

The proposed adaptation law and projection operator have the following properties [26] :

1) $\hat{W}(t)$ is uniformly continuous,
2) If $||\hat{W}(0)|| \leq W_M$, then $||\hat{W}(t)|| \leq W_M$, $\forall t > 0$,
3) $||\text{Proj}(y, \hat{W})|| \leq ||y||$,
4) $\tilde{W}^T\text{Proj}(y, \hat{W}) \leq \tilde{W}^T y$,
5) $||\text{Proj}(y, \hat{W})||$ is bounded if $||y||$ is also bounded.

Applying the adaptive control torque (15) to the AAFO system modeled by (1), the dynamics of the closed loop system can be determined :

$$J\dot{s} = -\tilde{W}Y^T - \alpha_p \text{sat}_{N_1}(k_p\tilde{\theta}) - \alpha_v \text{sat}_{N_2}(k_v\dot{\tilde{\theta}}) + \tau_h - \hat{J}\hat{d}$$

which is equivalent to :

$$J\dot{s} = -\tilde{W}Y^T - \alpha_p \text{sat}_{N_1}(k_p\tilde{\theta}) - \alpha_v \text{sat}_{N_2}(k_v\dot{\tilde{\theta}}) + \hat{J}\tilde{d} + \tilde{f} \tag{19}$$

IV. STABILITY ANALYSIS

The stability of the wearer-AAFO system subject to the projection-based adaptive controller together with nonlinear disturbance observer is analyzed in this section.

Proposition 2: Consider the AAFO system modeled by (1). Suppose that the current and desired ankle joint angles and their derivatives up to the second order are bounded (Assumption 1). Applying the control torque (15, 17) with the external input torque estimated by means of the NDOB (10) ensures that the trajectories of the system $\tilde{x} = [\tilde{\theta},\ \dot{\tilde{\theta}}]^T = [0,\ 0]^T$ remain uniformly ultimately bounded.

Proof: Consider the Lyapunov function V defined by :

$$V = \frac{1}{2}Js^2 + \frac{1}{2}\tilde{W}^T\Gamma^{-1}\tilde{W} + \varepsilon\int_0^{\tilde{\theta}} \text{sat}_{N_1}(k_p x)dx \tag{20}$$

with $\Gamma = \text{diag}(a_i),\ i \in \{1, \ldots, 7\}$. The derivative of V is given by :

$$\dot{V} = sJ\dot{s} - \tilde{W}^T\Gamma^{-1}\dot{\hat{W}} + \varepsilon \text{sat}_{N_1}(k_p\tilde{\theta})\dot{\tilde{\theta}} \tag{21}$$

Replacing (17, 19) into (21), the derivative of the Lyapunov function V becomes :

$$\begin{aligned}
\dot{V} &= \underbrace{-\tilde{W}Y^T s + \tilde{W}\text{Proj}(Y^T s, \hat{W})}_{\leq 0} + \varepsilon \text{sat}_{N_1}(k_p\tilde{\theta})\dot{\tilde{\theta}} \\
&\quad -\left(\alpha_p \text{sat}_{N_1}(k_p\tilde{\theta}) + \alpha_v \text{sat}_{N_2}(k_v\dot{\tilde{\theta}})\right) s + (\hat{J}\tilde{d} + \tilde{f})s \\
&\leq -\begin{bmatrix}\tilde{\theta} & \dot{\tilde{\theta}}\end{bmatrix}\begin{bmatrix}\alpha_p\lambda & \alpha_v\lambda \\ \alpha_p - \varepsilon & \alpha_v\end{bmatrix}\begin{bmatrix}\text{sat}_{N_1}(k_p\tilde{\theta}) \\ \text{sat}_{N_2}(k_v\dot{\tilde{\theta}})\end{bmatrix} \\
&\quad +(\hat{J}\tilde{d} + \tilde{f})\begin{bmatrix}\lambda & 1\end{bmatrix}X \\
&\leq -X^T\Delta\text{Sat}_N(KX) + (\hat{J}\tilde{d} + \tilde{f})\Lambda X
\end{aligned}$$

where

$$\Delta = \begin{bmatrix}\alpha_p\lambda & \alpha_v\lambda \\ \alpha_p - \varepsilon & \alpha_v\end{bmatrix} \quad \text{and} \quad \Lambda = \begin{bmatrix}\lambda & 1\end{bmatrix}.$$

Λ and $K = \text{diag}(k_p, k_v)$ are two matrices positive definite, $X = [\tilde{\theta}\ \ \dot{\tilde{\theta}}]^T$, $N = [N_1\ \ N_2]^T$, and

$\text{Sat}_B(\Phi) = [\text{sat}_{B_1}(\phi_1)\ \text{sat}_{B_2}(\phi_2)\ \dots\ \text{sat}_{B_n}(\phi_n)]^T$ with $\Phi = [\phi_1\ \phi_2\ \dots\ \phi_n]^T$, $B = [B_1\ B_2\ \dots\ B_n]^T$, and $n \in \mathbb{N}$.

X_i^T and $\text{Sat}_N(K_{(i,i)}X_i)$, $i \in \{1,2\}$, have the same sign, $\lambda_{\min}(\cdot)$ and $\lambda_{\max}(\cdot)$ are respectively the minimum and maximum eigenvalues of the embedded matrices.

$X^T\Delta\text{sat}(KX)$ is then positive and can be bounded by :

$$\lambda_{\min}(\Delta)\lambda_{\min}(K)\|X\|^2 \leq X^T\Delta\text{sat}(KX) \leq \lambda_{\max}(\Delta)N\|X\|$$

The derivative of the Lyapunov function becomes :

$$\begin{aligned}\dot{V} &\leq -\lambda_{min}(\Delta)\lambda_{min}(K)\|X\|^2 + |\hat{J}\tilde{d} + \tilde{f}|\sqrt{1+\lambda^2}\|X\| \\ &\leq -\delta\|X\|^2 + |\hat{J}\tilde{d} + \tilde{f}|\sqrt{1+\lambda^2}\|X\| \end{aligned} \quad (22)$$

where $\delta = \lambda_{\min}(\Delta)\lambda_{min}(K)$.

Taking $0 < m < 1$, the derivative of the Lyapunov function can be bounded by :

$$\dot{V} \leq -\delta(1-m)\|X\|^2 - m\delta\|X\|^2 + |\hat{J}\tilde{d} + \tilde{f}|\sqrt{1+\lambda^2}\|X\|$$

and therefore :

$$\dot{V} \leq -\delta(1-m)\|X\|^2 \quad \forall\|X\| \geq \frac{|\hat{J}\tilde{d} + \tilde{f}|\sqrt{1+\lambda^2}}{m\delta} \quad (23)$$

$\frac{(\hat{J}\tilde{d}+\tilde{f})\sqrt{1+\lambda^2}}{m\delta}$ vanishes if $(\hat{J}\tilde{d}+\tilde{f})$ vanishes. $\|X\|$ is bounded by μ, where $\mu = \frac{B\sqrt{1+\lambda^2}}{m\delta}$ and $B = W_M\sqrt{2\epsilon} + B_f$. Therefore,

$$\dot{V} < 0 \quad \forall\ X \text{ such that } \|X\| \geq \mu. \quad (24)$$

Which means that the Lyapunov function V is decreasing outside the set defined by $\{\|X\| \leq \mu\}$. From (20), one can notice that V is bounded by :

$$V \leq \alpha_1\|X\|^2 + \alpha_2\|X\| + \beta$$

where $\alpha_1 = \frac{1}{2}J(1+\lambda^2)$, $\alpha_2 = \varepsilon N_1$ and $\beta = \frac{1}{2}\lambda_{\max}(\Gamma^{-1})W_M^2$. Choosing $c > \eta$ where $\eta = \alpha_1\mu^2 + \alpha_2\mu + \beta$, the derivative of the Lyapunov function $\dot{V}$ is negative on the boundary $V = c$. The solutions starting in the set $\{V \leq c\}$ will remain therein for all future time. For any ξ such that $\eta < \xi < c$, $\dot{V}$ will be negative in the set $\{\xi < V < c\}$ and V will decrease monotonically until the solutions enter the set $\{V \leq \xi\}$ and cannot leave it anymore after because $\dot{V}$ is negative on the boundary $V = c$. Therefore the solutions are uniformly ultimately bounded. ■

V. EXPERIMENTAL RESULTS

A. Experimental setup

The experiments were performed using an actuated ankle foot orthosis (AAFO) of the left leg. The AAFO is driven by a DC motor coupled to a gearbox to ensure dorsiflexion and plantar-flexion of the ankle joint. It is equipped by an incremental encoder that measures the angle θ between the foot and the shank. Each insole is equipped by three force-sensitive resistor (FSR) sensors that measure the ground reaction forces when the foot is in contact with the ground. Two Inertial Measurement Units (IMU) are used : the first one is placed at the shank and is used to calculate the angle between the shank and the vertical axis θ_s and contributes at the same time, to the detection of the IC gait event FIG. 2. The second IMU is placed at the foot to measure the linear acceleration of the wearer along the three axes. Two surface-Electromyography (SEMG) sensors were placed respectively on the Tibialis Anterior (TA) and the Gastrocnemius Medialis (GM) muscles to measure the muscular activity. The angular velocity of the ankle joint $\dot{\theta}$ is derived and filtered numerically with a lowpass, fourth order Butterworth filter (cutoff frequency of 20Hz). The electronics / calculator and the battery are packaged in a banana bag fastened around the waist without constraining the wearer.

B. Experimental Protocol

Three healthy subjects have participated in the experiments. They do not present any spasticity and are able to perform full plantar flexion and full dorsiflexion. The subjects were informed of the progress of the tests, the instrumentation included in the protocol and the outcome of the study. They gave their written consent before participating in the experiments. Table I gives some information about the subjects.

TABLE I – Information about the three participants to the experiments

Subject	Age	Sex	Height (cm)	Weight (kg)
A	21	M	177	75
B	25	M	185	85
C	25	M	180	77

The experimental protocol is described as follows : prior to each walking session, five gait cycles were used to calibrate the adaptive reference generation algorithm. For each subject, a set of three unassisted sessions were recorded first, then, the control torque was applied to the AAFO and three assisted sessions were recorded. The subject wearing the AAFO walked on a treadmill for one minute at a fixed velocity of 2 Km/h. The subjects had one minute of rest between each session.

C. Results

The tuning gains Γ_i have been set to : Γ_1=Γ_2=Γ_3=Γ_4=Γ_5=Γ_7=0.001, and Γ_6=0.00001. The controller's gains have been set to $\alpha_p = 1$ and $\alpha_v = 1$ with the saturation bounds $N_1 = N_2 = 10$ and the gains $\lambda = 1$, $k_p = 6$ and $k_v = 1$. The observer's gain was set to $L = 0.01$. All the adaptive parameters were initialized to zero except for $\hat{J}_0 = 0.001$, and the ankle joint angle at the rest position has been taken as $\theta_r = \frac{\pi}{2}$. These values were obtained by trial and error, which allows a compromise between tracking accuracy and the comfort of the wearer.

FIG. 3 shows the tracking performance for Subject A during the first 30 seconds of the experiment, a positive torque indicates a dorsiflexion assistance whereas a negative one provides plantar flexion assistance. It can be seen that the estimated disturbances converged to its steady form after nearly 15 seconds which is suitable for the time of the experiment. The same time was needed for the estimated

parameters to converge as shown in FIG. 4. Recall that these values are not an estimation of the true parameters of the system (Remark 2). The root mean square error (RMSE) of the trajectory tracking angle and angular velocity for all three subjects is shown in FIG. 5. Both angle and angular velocity errors were significantly reduced when the wearers were assisted. In FIG. 6, the mean absolute assistive torques per cycle for all subjects are shown. It was calculated by integrating the absolute value of the assistive torque for all sessions. Table II shows the average estimated parameters and their standard deviation for the last 10 seconds of of the experiment. The low standard deviation verifies the convergence of the estimated parameters for all subjects.

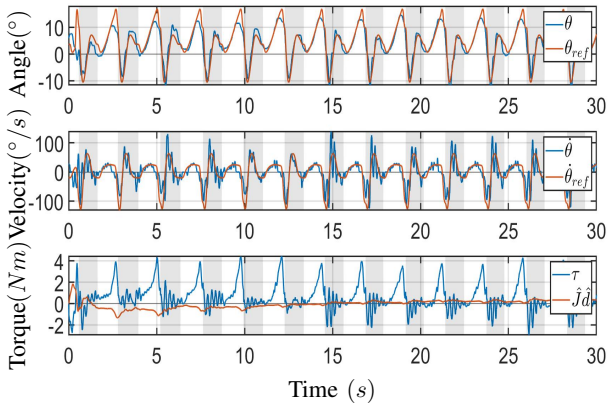

FIG. 3 – Subject A. System's performance tracking the desired ankle joint angle profile during the first 30s of the experiment. In the first two plots, the red line represents the reference profile and the blue line is the current trajectory for both the ankle joint angle and angular velocity. In the bottom plot, the red line is the estimated disturbance torque ($\hat{J}\hat{d} = \tau_h - \hat{f}$) and the blue line is the applied assistive one. For all plots, the grey area represent the swing phase whereas the white one is the stance.

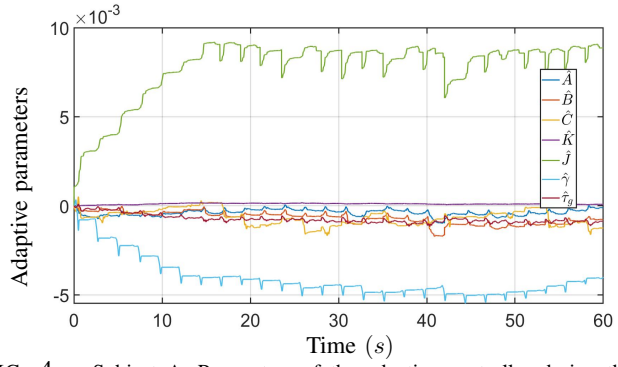

FIG. 4 – Subject A. Parameters of the adaptive controller during the assisted session.

TABLE II – The mean values and standard deviations of the estimated parameters, relative to the three subjects, averaged for the last 10s of the experiments (values $\times 10^{-4}$).

	A	B	C
$\hat{A}(Nm)$	-3.87±1.5	-13±2.93	-5.42±2.13
$\hat{B}(Nm.s/rad)$	-9.34±1.47	-11±3.41	-3.96±4.16
$\hat{C}(Ns^2)$	-7.65±4.81	-6.27±5.46	-1.1±2.3
$\hat{K}(Nm/rad)$	0.82±0.13	1.23±0.24	0.38±0.12
$\hat{J}(Nm.s^2/rad)$	87±3.7	50±8.68	1.1±0.28
$\hat{\gamma}$	-45±3	-84±3.67	-98±1.97
$\hat{\tau}_g(Nm)$	-9±0.82	-1.66±0.98	-0.91±0.75

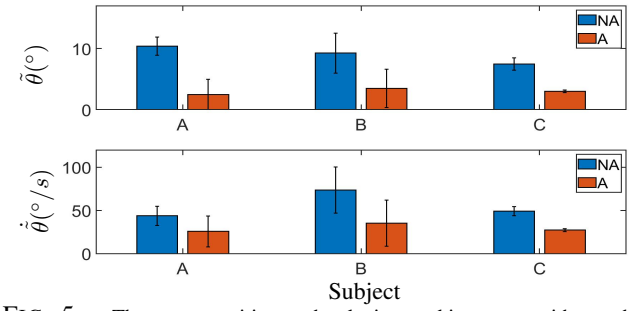

FIG. 5 – The mean position and velocity tracking error with standard deviations for the three subjects when they were not assisted (NA) then assisted (A) by the AAFO.

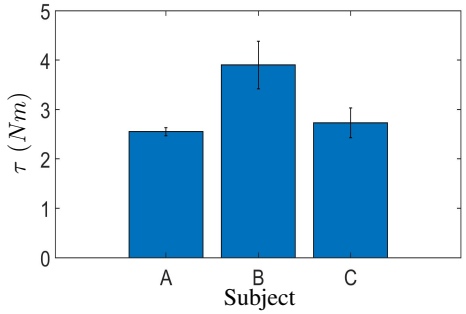

FIG. 6 – The absolute assistive torque per cycle with standard deviations provided by the AAFO for the three subjects.

VI. CONCLUSIONS AND FUTURE WORKS

This paper presents an adaptive active disturbance rejection control intended to assist paretic patients during their rehabilitation process. A NDOB is used to estimate disturbances resulting from the human torque and the parameters estimation error. An adaptive controller coupled to the human muscular torque rejection term ensured the tracking of an adaptive desired trajectory. As far, the controller and observer's performances have been tested in real time with three healthy subjects using the AAFO of the LISSI-lab. Results have shown fast and satisfactory convergence of the estimated external torque and the current ankle profile towards the desired one. Ongoing works are focusing particularly on testing the proposed controller with paretic patients in a clinical environment. Future works will concern the development of hybrid control strategies including functional electrical stimulation along with the AAFO to further promote the subject involvement in the task achievement.

REFERENCES

[1] S. Roelker, M. Bowden, S. Kautz, and R. Neptne, "Paretic propulsion as a measure of walking performance and functional motor recovery post-stroke : A review," *Gait & Posture*, vol. 68, pp. 6–14, 2019.

[2] S. Mohammed, Y. Amirat, and H. Rifai, "Lower limb movement assistance through wearable robots : State of the art and challenges," *Advanced Robotics*, vol. 26, no. 1-2, pp. 1–22, 2012.

[3] C. Thalman, T. Hertzell, and H. Lee, "Toward a soft robotic ankle-foot orthosis (sr-afo) exosuit for human locomotion : Preliminary results in late stance plantarflexion assistance," in *IEEE International Conference on Soft Robotics (RoboSoft)*, 2020, pp. 801–807.

[4] U. Martinez-Hernandez, A. Rubio-Solis, V. Cedeno-Campos, and A. Dehghani-Sanij, "Towards an intelligent wearable ankle robot for assistance to foot drop," in *IEEE International Conference on Systems, Man and Cybernetics*, 2019, pp. 3410–3415.

[5] J. Kwon, J. Park, S. Ku, Y. Jeong, N. Paik, and Y. Park, "A soft wearable robotic ankle-foot-orthosis for post-stroke patients," *IEEE Robotics & Automation Letters*, vol. 4, no. 3, pp. 2547–2552, 2019.

[6] R. Silva, A. Veloso, N. Alves, C. Fernandes, and P. Morouço, "A review of additive manufacturing studies for producing customized ankle-foot orthoses," *Bioengineering*, vol. 9, no. 249, 2022.

[7] K. E. Gordon, C. R. Kinnaird, and D. P. Ferris, "Locomotor adaptation to a soleus EMG-controlled antagonistic exoskeleton," *Journal of Neurophysiology*, vol. 109, no. 7, pp. 1804–1814, 2013.

[8] J. Pérez-Ibarra and A. Siqueira, "Comparison of kinematic and EMG parameters between unassisted, fixed-and adaptive-stiffness robotic-assisted ankle movements in post-stroke subjects," in *International conference on rehabilitation robotics (ICORR)*, London, UK, 2017, p. 461–466.

[9] J. Furukawa, T. Noda, T. Teramae, and J. Morimoto, "Human movement modeling to detect biosignal sensor failures for myoelectric assistive robot control," *Transactions on Robotics*, vol. 33, no. 4, pp. 846–857, 2017.

[10] J. Blaya and H. Herr, "Adaptive control of a variable impedance ankle-foot orthosis to assist drop-foot gait," *Transactions on Neural systems and Rehabilitation Engineering*, vol. 12, no. 1, pp. 24–31, 2004.

[11] A. Roy, H. krebs, J. Barton, N. Macko, and L. Forrester, "Anklebot-assisted locomotor training after stroke : A novel deficit-adjusted control approach," in *International Conference on Robotics and Automation (ICRA)*, 2013, pp. 2175–2182.

[12] A. Roy, H. krebs, K. Iqbal, R. Macko, N.R. Macko, and L. Forrester, "Facilitating push-off propulsion : A biomechanical modelof ankle robotics assistance for plantar flexion gait training in stroke," in *International Conference on Biomedical Robotics and Biomechatronics*, 2014, pp. 656–663.

[13] M. Lawn, M. Takashima, J. Ninomiya, M. Yu, K. Soma, and T. Ishimatsu, "Development of an actuation system for a rotary hydraulic brake on a low cost light weight knee-ankle-foot orthosis," in *IEEE Sensors*, Busan, South Korea, 2015, pp. 1–4.

[14] J. Pérez-Ibarra, A. Siqueira, M. Silva-Couto, T. de Russo, and H. Krebs, "Adaptive impedance control applied to robot-aided neuro-rehabilitation of the ankle," *IEEE Robotics and Automation Letters*, vol. 4, no. 2, pp. 185–192, 2019.

[15] J. Ward, T. Sugar, J. Standeven, and J. R. Engsberg, "Stroke survivor gait adaptation and performance after training on a powered ankle foot orthosis," in *International Conference on Robotics and Automation (ICRA)*, Anchorage, AK, USA, 2010, pp. 211–216.

[16] *Mathematical Methods in Engineering*. Springer, Dordrecht, 2014, ch. Adaptive System for Control of Active Ankle-Foot Orthosis and Gait Analysis, pp. 153–163.

[17] M. Zhang, J. Cao, S. Xie, G. Zhu, X. Zeng, X. Huang, and Q. Xu, "A priliminary study on robot-assisted ankle rehabilitation for the treatment of drop foot," *Journal of Intelligent and Robotic systems*, vol. 91, no. 2, pp. 207–215, 2018.

[18] J. Guerrero-Castellanos, H. Rifaï, V. Arnez-Paniagua, J. Linares-Flores, L. Saynes-Torres, and S. Mohammed, "Robust active disturbance rejection control via control lyapunov functions : Application to actuated-ankle–foot-orthosis," *Control Engineering Practice*, vol. 80, pp. 49–60, 2018.

[19] V. Arnez-Paniagua, H. Rifai, Y. Amirat, M. Ghedira, J. Gracies, and S. Mohammed, "Adaptive control of an actuated ankle-foot orthosis for paretic patients," *Control Engineering Practice*, vol. 90, pp. 207–220, 2019.

[20] T. Johnston, S. Keller, C. Denzer-Weiler, and L. A. Brown, "Clinical practice guideline for the use of ankle-foot orthoses and functional electrical stimulation post-stroke," *Journal of Neurologic Physical Therapy*, vol. 45, no. 2, pp. 112–196, 2021.

[21] D. Winter, *Biomechanics and motor control of human movement*, 4^{th} ed., Wiley, Ed. John Wiley & Sons, 2009.

[22] V. Arnez-Paniagua, W. Huo, I. Colorado-Cervantes, S. Mohammed, and Y. Amirat, "A hybrid approach towards assisting ankle joint of paretic patients," in *Proc. of the 20th International Functional Electrical Stimualtion Society Conference*, La Grande-Motte, France, 2016.

[23] K. Kong and M. Tomizuka, "A gait monitoring system based on air pressure sensors embedded in a shoe," *Transactions on mechatronics*, vol. 14, no. 3, pp. 358–370, 2009.

[24] E. Hutin, D. Pradon, F. Barbier, B. Bussel, J.-M. Gracies, and N. Roche, "Walking velocity and lower limb coordination in hemiparesis," *Gait & posture*, vol. 36, no. 2, pp. 205–211, 2012.

[25] G. S. Natal, A. Chemori, and F. Pierrot, "Nonlinear control of parallel manipulators for very high accelerations without velocity measurement : stability analysis and experiments on par2 parallel manipulator," *Robotica*, vol. 34, no. 1, pp. 43–70, 2016.

[26] G. Satori-Natal, A. Chemori, and F. Pierrot, "Nonlinear control of parallel manipulators for very high accelerations without velocity measurement : stability analysis and experiments on par2 parallel manipulator," *Robotica*, pp. 1–28, 2014.